Tumor and Stem Cell Biology

Cancer Research

ETS Transcription Factor ESE1/ELF3 Orchestrates a Positive Feedback Loop That Constitutively Activates NF-κB and Drives Prostate Cancer Progression

Nicole Longoni[1], Manuela Sarti[1], Domenico Albino[1], Gianluca Civenni[1], Anastasia Malek[1], Erica Ortelli[1], Sandra Pinton[1], Maurizia Mello-Grand[3], Paola Ostano[3], Gioacchino D'Ambrosio[4], Fausto Sessa[4,5], Ramon Garcia-Escudero[6], George N. Thalmann[2], Giovanna Chiorino[3], Carlo V. Catapano[1], and Giuseppina M. Carbone[1]

Abstract

Chromosomal translocations leading to deregulated expression of ETS transcription factors are frequent in prostate tumors. Here, we report a novel mechanism leading to oncogenic activation of the ETS factor ESE1/ELF3 in prostate tumors. ESE1/ELF3 was overexpressed in human primary and metastatic tumors. It mediated transforming phenotypes *in vitro* and *in vivo* and induced an inflammatory transcriptome with changes in relevant oncogenic pathways. ESE1/ELF3 was induced by interleukin (IL)-1β through NF-κB and was a crucial mediator of the phenotypic and transcriptional changes induced by IL-1β in prostate cancer cells. This linkage was mediated by interaction of ESE1/ELF3 with the NF-κB subunits p65 and p50, acting by enhancing their nuclear translocation and transcriptional activity and by inducing p50 transcription. Supporting these findings, gene expression profiling revealed an enrichment of NF-κB effector functions in prostate cancer cells or tumors expressing high levels of ESE1/ELF3. We observed concordant upregulation of ESE1/ELF3 and NF-κB in human prostate tumors that was associated with adverse prognosis. Collectively, our results define an important new mechanistic link between inflammatory signaling and the progression of prostate cancer. *Cancer Res; 73(14); 4533–47. ©2013 AACR.*

Introduction

Prostate cancer is the most common form of cancer in men and a leading cause of cancer-related death in western countries (1). Deregulation of ETS transcription factors is very frequent in prostate cancer, suggesting that the prostate epithelium might be highly sensitive to unbalanced expression of these transcription factors (2, 3). About 50% of prostate tumors harbor chromosomal translocations leading to overexpression of ETS genes, such as *ERG*, *ETV1*, and *ETV4* (2, 4). ETS transcription factors, including ESE3/EHF and ETV1, are also frequently deregulated in prostate tumors and other tumor types despite the absence of chromosomal rearrangements (5–9). In this study, we report a novel mechanism leading to overexpression and oncogenic activation of an additional ETS transcription factor, ESE1/ELF3, in both primary and metastatic prostate cancers. ESE1/ELF3 is a member of the epithelial-specific subfamily of ETS transcription factor and has been reported to be involved in a variety of pathophysiologic processes, including cancer and inflammatory disorders (10–12). However, the role of ESE1/ELF3 in prostate tumorigenesis is unknown. We found that ESE1/ELF3 functions at the crossroad between cancer and chronic inflammation to promote prostate cancer progression. Epidemiologic, genetic, and histopathologic studies strongly support a connection between chronic inflammation and prostate cancer (13). However, the molecular mechanisms linking chronic inflammation and prostate tumorigenesis are still unclear. Production of proinflammatory cytokines, such as interleukin (IL)-1β, and constitutive activation of NF-κB play an important role in cancer-associated inflammation and tumorigenesis (14–19). We found that ESE1/ELF3 is a target of IL-1β and NF-κB in prostate cancer cells and an essential element in a positive feedback loop sustaining constitutive activation of NF-κB in prostate tumors. We provide evidence that this positive feedback loop is active in human prostate tumors and is associated with aggressive disease and adverse prognosis. These data thus provide the rationale for patient risk stratification and context-dependent therapeutic strategies in a specific subset of patients with prostate cancer.

Authors' Affiliations: [1]Institute of Oncology Research (IOR), Oncology Institute of Southern Switzerland (IOSI), Bellinzona; [2]Urology Research Laboratory, Department of Urology, University of Bern, Inselspital, Bern, Switzerland; [3]Laboratory of Cancer Genomics, Fondazione Edo ed Elvo Tempia Valenta, Biella; [4]IRCCS Multimedica, Milan; [5]Department of Pathology University of Insubria, Varese, Italy; and [6]Molecular Oncology Unit, CIEMAT, Madrid, Spain

Note: Supplementary data for this article are available at Cancer Research Online (http://cancerres.aacrjournals.org/).

Corresponding Author: Giuseppina M. Carbone, Institute of Oncology Research (IOR), Oncology Institute of Southern Switzerland (IOSI), Via Vela 6, Bellinzona 6500, Switzerland. Phone: 41-91-820-0366; Fax: 41-91-820-0397; E-mail: pina.carbone@ior.iosi.ch

doi: 10.1158/0008-5472.CAN-12-4537

Materials and Methods

Cell culture, cell transfection, and selection of stable cell clones

LNCaP, 22RV1, and DU145 were obtained from American Type Culture Collection and maintained in RPMI-1640 supplemented with 10% FBS. Immortalized prostate epithelial cells (LHS) were maintained in prostate epithelial cell growth medium (PrEGM; Cambrex, Lonza Group Ltd.) as previously described (5, 7). ESE1/ELF3–expressing polyclonal stable cell lines were generated by transfection of the pESE1/ELF3–expressing vector [kindly provided by Dr. T. Libermann (Beth Israel Deaconess Medical Center, Boston, MA; ref. 10), and negative control cells were obtained by transfection with pcDNA3.1, as previously described (5, 7). For transient ESE1/ELF3 gene knockdown, cells were transfected with siRNAs directed to the exon 3 (siESE1) or to the 3′-untranslated region (UTR; si3′-UTR; Ambion) and control siRNA directed to the firefly luciferase gene (*siGL3*) using Lipofectamine 2000 (Invitrogen). Luciferase reporter assays were conducted as previously described (5, 7) using the pGL4.32(luc2P/NF-κB-RE/Hygro) vector (Promega AG). For IL-1β treatment, cells were seeded in 6-wells plates and treated after 24 hours with IL-1β (Sigma-Aldrich Chemie GmbH) diluted in 0.1% bovine serum albumin in PBS.

Cell proliferation, anoikis, and cell migration

Cell growth, clonogenic, and anoikis assays were conducted as previously described (5, 7). The scratch/wound healing and Boyden chamber assays were conducted and analyzed as previously described (7).

RNA extraction and quantitative RT-PCR

Total RNA was extracted and quantitative real time PCR (qRT-PCR) was conducted using custom made primers (Supplementary Table S1) and analyzed as previously described (5).

Immunoblotting from cells and tumor xenografts

Cell lysates were prepared and analyzed as described previously (5, 7). Antibodies against ESE1/ELF3 (ab1392; Abcam), p50, p65, β-tubulin (Calbiochem), glyceraldehyde-3-phosphate dehydrogenase (GAPDH), and histone H3 (Millipore AG) were obtained from the indicated sources. Lysate from tumor xenografts were prepared from freshly frozen tissue. Cytoplasmic and nuclear extracts were obtained using NE-PER Nuclear and Cytoplasmic Extraction Reagent (Thermo Scientific).

Immunoprecipitation

Immunoprecipitation was conducted as previously described (20). Cell lysates were incubated with antibodies against ESE1/ELF3 and p50. Immunoblotting was conducted using antibodies against ESE1/ELF3, p50, and p65.

Immunofluorescence and fluorescence microscopy

Cells were grown on glass coverslips, as previously described (20) and incubated with antibodies for ESE1/ELF3, p50, and p65 followed by incubation with anti-rabbit Alexa Fluor 488 or anti-mouse Alexa Fluor 594 (Invitrogen) secondary antibodies. Pictures were taken as previously described (20).

Chromatin immunoprecipitation

Chromatin immunoprecipitation (ChIP) was carried out and analyzed using quantitative real-time PCR as previously described (5, 7). ChIP from fresh-frozen prostate tumors was conducted as previously described (5, 7).

Animal studies

Mice were purchased from the Harlan Laboratories. Study protocols were approved by the Swiss Veterinary Authority (No. 5/2011). For subcutaneous tumor xenografts, 1×10^6 cells were inoculated in the flank of athymic male nude mice (Balb c nu/nu; $n = 10$/group). Tumor size was monitored twice a week with a caliper. To assay lung metastases, 1×10^6 cells were injected into tail vein of athymic male nude mice twice with a 24-hour interval between injections. Animals were sacrificed after 4 weeks. Lungs were collected and a quantitative real-time PCR–based method that relies on selective amplification of species-specific, unique, untranslated, and conserved regions of the human and mouse genome was used to quantify the percentage of human metastatic cells in mouse lungs (21).

Gene expression profiling

RNA from cell lines was amplified, labeled, and hybridized as described (5). Significantly modulated transcripts were selected by applying 0.01 as cutoff for the adjusted *P* value (Benjamini–Hochberg correction) and 1 as cutoff for the log fold-change. Data are MIAME (Minimum Information About a Microarray Gene Experiment) compliant and have been deposited in the Gene Expression Omnibus: GEO accession numbers GSE39668.

Functional annotation and transcription factor interactome analysis

For functional annotation, gene lists were uploaded into the Database for Annotation, Visualization and Integrated Discovery (DAVID; http://david.abcc.ncifcrf.gov/summary.jsp). Enrichment of transcription factors interactome analysis was done using MetaCore version 6.10 (GeneGo Inc.) and Chip Enrichment Analysis (ChEA).

Gene set enrichment analysis

Gene set enrichment analysis (GSEA) was conducted as previously described (7). For all the datasets, the comparison of ESE1/ELF3 high versus all other tumors was conducted; for the Biella dataset, the tumor versus normal tissue comparison was also made. The following gene lists were used for GSEA: GS_3: Human NF-κB Signaling Targets; GS_5: Genes upregulated in 22RV1-pESE1 cells versus 22RV1-pcDNA.

Immunohistochemistry

Tissue microarrays (TMA) were constructed from formalin-fixed paraffin-embedded tissue specimens as previously described (7, 22). Tissue samples were collected with the approval of the Institutional Ethics Committees (IRCCS Multimedica of the Regione Lombardia, IT, and Insespital, Bern,

Switzerland) and patient written-informed consent. Immunohistochemistry (IHC) was conducted using antibodies against ESE1/ELF3 (ab1392; Abcam), p50 (E-10) sc-8414, and p65 (C-20) sc-372 (Santa Cruz Biotechnology). Two trained investigators scored the slides and were blinded to the study endpoints. At least 2 investigators scored the slides and were blinded to the study endpoints. Score was based on the percentage of ESE1/ELF3–positive cells: low, $\leq$20%; intermediate, >20% to <60%; high, $\geq$60%.

Survival analysis

Kaplan–Meier survival curves of patients groups were created using survplot package of R environment.

Results

ESE1/ELF3 is overexpressed in human prostate cancers

Using qRT-PCR, we found that primary tumors ($n = 65$) had significantly increased *ESE1/ELF3* mRNA level ($P = 3.17E{-}04$) compared with normal prostate tissue ($n = 14$). As previously reported (5), *ESE1/ELF3* was one of the most frequently deregulated ETS genes in prostate tumors. Specifically, 27% and 24% of tumors had, respectively, intermediate and high level of expression (Fig. 1A). Consulting additional patient microarray datasets (23, 24), we found further evidence of *ESE1/ELF3* overexpression in prostate tumors (Fig. 1A and Supplementary Fig. S1A). Furthermore, the level of *ESE1/ELF3* was significantly higher ($P < 0.001$) in metastatic tumors compared with primary tumors in 2 distinct datasets (Fig. 1B), suggesting an association of *ESE1/ELF3* upregulation with tumor progression. Notably, we found also evidence of amplification of the *ESE1/ELF3* gene locus in 3 prostate cancer datasets with a frequency of 2% to 6% using cancer outlier profile analysis (COPA) of DNA (Fig. 1C). To support these findings, ESE1/ELF3 protein expression was evaluated by IHC in a total of 207 primary tumors and 28 normal prostate samples in TMAs from 2 patient cohorts (7). ESE1/ELF3 was detected in the cytoplasm and nuclei of prostate epithelial cells both in normal and cancer tissue (Fig. 1D). Consistent with gene expression data, ESE1/ELF3 protein level was low in normal prostate and in about a third of tumors. In contrast, 35% and 28% of tumors had, respectively, intermediate and high levels of expression. Collectively, the high frequency of overexpression at the RNA and protein level, along with the evidence of amplification, strongly supported an oncogenic role of ESE1/ELF3 in prostate cancer. Interestingly, when we analyzed the relationship between *ESE1/ELF3* and *ERG*, the most frequently rearranged ETS gene, in patients samples previously evaluated by qRT-PCR (5), we found that *ESE1/ELF3* upregulation occurred independently of *ERG* overexpression (Supplementary Fig. S1B). On the other hand, *ESE1/ELF3* was elevated in about half of the *ERG*-positive tumors, indicating that the two alterations were not mutually exclusive and could coexist in selected cases. A similar result was obtained by comparing ESE1/ELF3 and ERG protein expression by IHC (7), with 27% and 21% of tumors positive for either ESE1/ELF3 or ERG alone, respectively (Supplementary Fig. S1C).

ESE1/ELF3 contributes to the malignant phenotype of prostate cancer cells

To understand the biologic consequences of increased expression of *ESE1/ELF3*, we generated 22RV1 and LNCaP prostate cancer cell lines with stable expression of *ESE1/ELF3*. LNCaP cells are *ETV1* translocation–positive (25), whereas 22RV1 cells are ETS translocation–negative (26). LNCaP and 22RV1 cells have, respectively, low and intermediate level of *ESE1/ELF3* (Supplementary Fig. S2A). Stable polyclonal cell lines expressed high levels of *ESE1/ELF3* comparable with the level observed in high expressing prostate tumors and in DU145 cells, which have endogenously high level of *ESE1/ELF3* (Supplementary Fig. S2B–S2D), indicating that these cell lines could faithfully represent tumors with differential expression of *ESE1/ELF3*. Furthermore, ESE1/ELF3 in the stable overexpressing cells was localized in the nucleus and cytoplasm consistent with the distribution seen in prostate tissues (Supplementary Fig. S2C).

ESE1/ELF3–overexpressing cells exhibited greater ability to form colonies in soft agar (Fig. 1E), increased anoikis resistance (Fig. 1F), and cell migration (Fig. 1G and H) than parental cells, indicative of increased malignancy. Furthermore, ESE1/ELF3–overexpressing 22RV1 cells grew faster and formed significantly larger tumors than control cells when implanted subcutaneously in immunodeficient mice ($P < 0.05$; Fig. 1I). The 22RV1-pESE1 tumors xenografts expressed high level of ESE1/ELF3, similar to the level observed in high expressing human tumors (Supplementary Fig. S3). Upon intravenous injection, 22RV1-pESE1 cells produced large metastases in the lung detected by histopathology and immunohistochemical staining, whereas control 22RV1 cells did not (Fig. 1J, left). Consistently, using a highly sensitive quantitative real-time PCR method (21), we found a significantly higher load of human metastatic cells ($P < 0.05$) in the lung of mice injected with 22RV1-pESE1 cells compared with control 22RV1 cells (Fig. 1J, right). Therefore, ESE1/ELF3 overexpression conferred increased tumorigenicity and metastatic ability, consistent with a role in prostate cancer progression.

ESE1/ELF3 activates a proinflammatory and protumorigenic transcriptional program

To identify the gene network associated with ESE1/ELF3 upregulation, we conducted genome-wide transcriptome profiling in 22RV1-pESE1 and 22RV1-pcDNA cells. ESE1/ELF3 induced a robust signature with 602 upregulated and 270 downregulated genes ($P < 0.01$; $\log_2$ fold change > 1; Fig. 2A; Supplementary Table S2). Functional annotation analysis of the upregulated genes revealed enrichment of genes associated with relevant oncogenic pathways, including tissue development, migration, adhesion, and apoptosis (Fig. 2A). Interestingly, genes involved in the inflammatory response constituted one of the top functional groups among the genes induced in response to ESE1/ELF3 overexpression (Fig. 2A). Gene set enrichment analysis (GSEA) in a human prostate cancer microarray dataset revealed that the genes induced by ESE1/ELF3 in 22RV1-pESE1 cells were overrepresented in prostate tumors compared with normal tissue (Fig. 2B), suggesting that they were biologically relevant to prostate

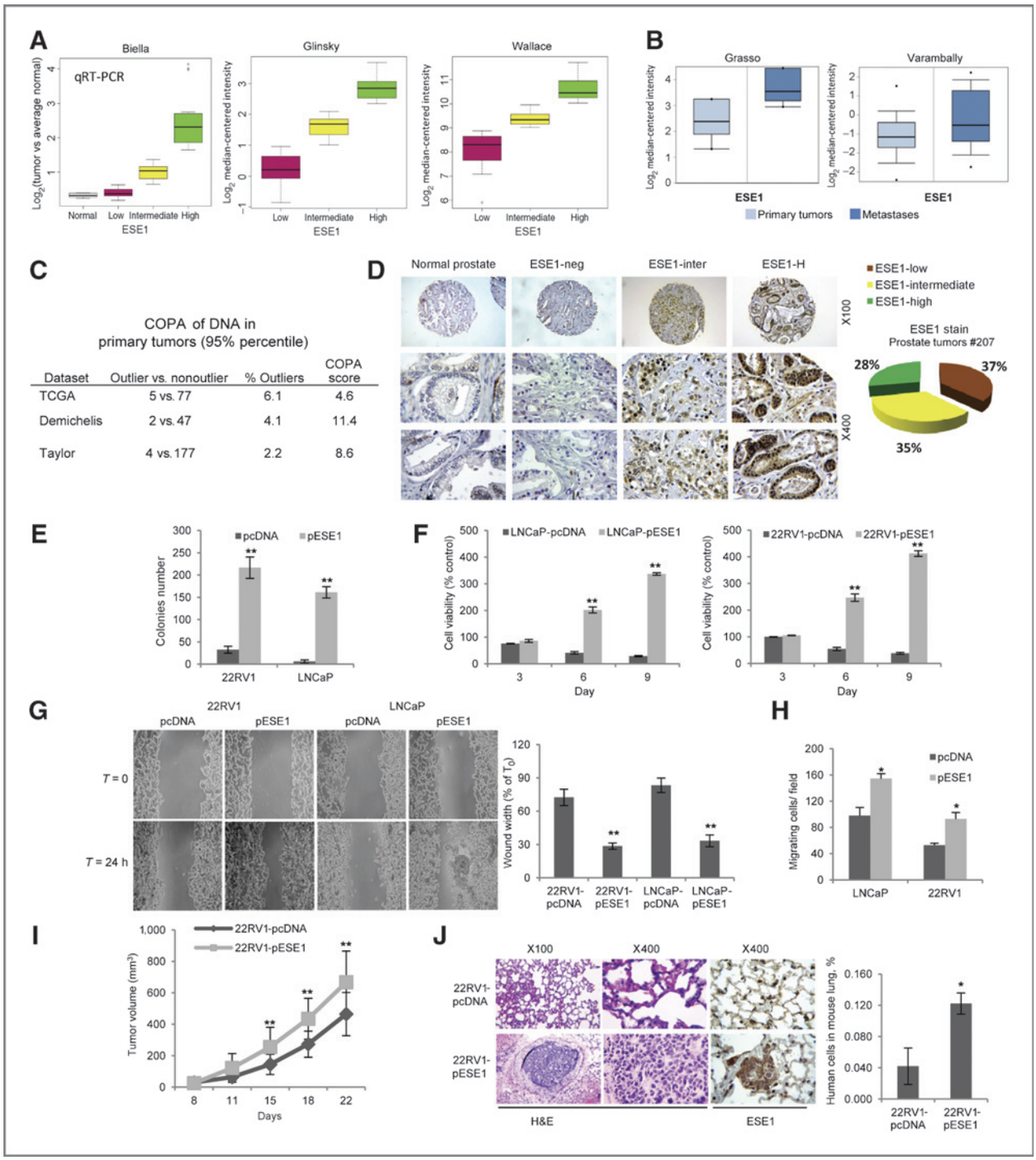

Figure 1. ESE1/ELF3 is overexpressed in prostate cancers and promotes malignant phenotypes. A, left, ESE1/ELF3 mRNA level in prostate tumors in the Biella patient cohort determined by qRT-PCR. Middle and right, level of ESE1/ELF3 in primary tumors in the indicated datasets evaluated by microarrays. B, level of ESE1/ELF3 in primary tumors versus metastases in the indicated datasets ($P < 0.001$). C, ESE1/ELF3 amplification in primary prostate tumors from 3 published datasets. TCGA, The Cancer Genome Atlas. D, immunohistochemical determination of ESE1/ELF3 protein in normal prostate and prostate tumors. Left, representative images; right, distribution based on immunohistochemical score in prostate tumors. E, colony formation in soft agar of control (pcDNA) and ESE1/ELF3–overexpressing (pESE1) 22RV1 and LNCaP cells. F, survival in anoikis of control (pcDNA) and ESE1/ELF3–overexpressing (pESE1) 22RV1 (right) and LNCaP (left) cells. G, scratch wound-healing assay with control (pcDNA) and ESE1/ELF3–overexpressing (pESE1) 22RV1 and LNCaP cells. Left, representative images. Right, percentage of wound width relative to time 0. H, Boyden chamber assay with control (pcDNA) and ESE1/ELF3–overexpressing (pESE1) 22RV1 and LNCaP cells. I, growth of subcutaneous xenografts ($n = 10$/group) of 22RV1-pcDNA and 22RV1-pESE1 cells in nude mice. J, formation of lung metastasis upon tail vein injection of 22RV1-pcDNA and 22RV1-pESE1 cells. Left, representative images of lung sections stained with H&E and for ESE1/ELF3. Right, PCR quantification of human metastatic cells in mouse lungs. *P* values were determined using *t* test. *, $P < 0.01$; **, $P < 0.005$. All data are mean ± SEM.

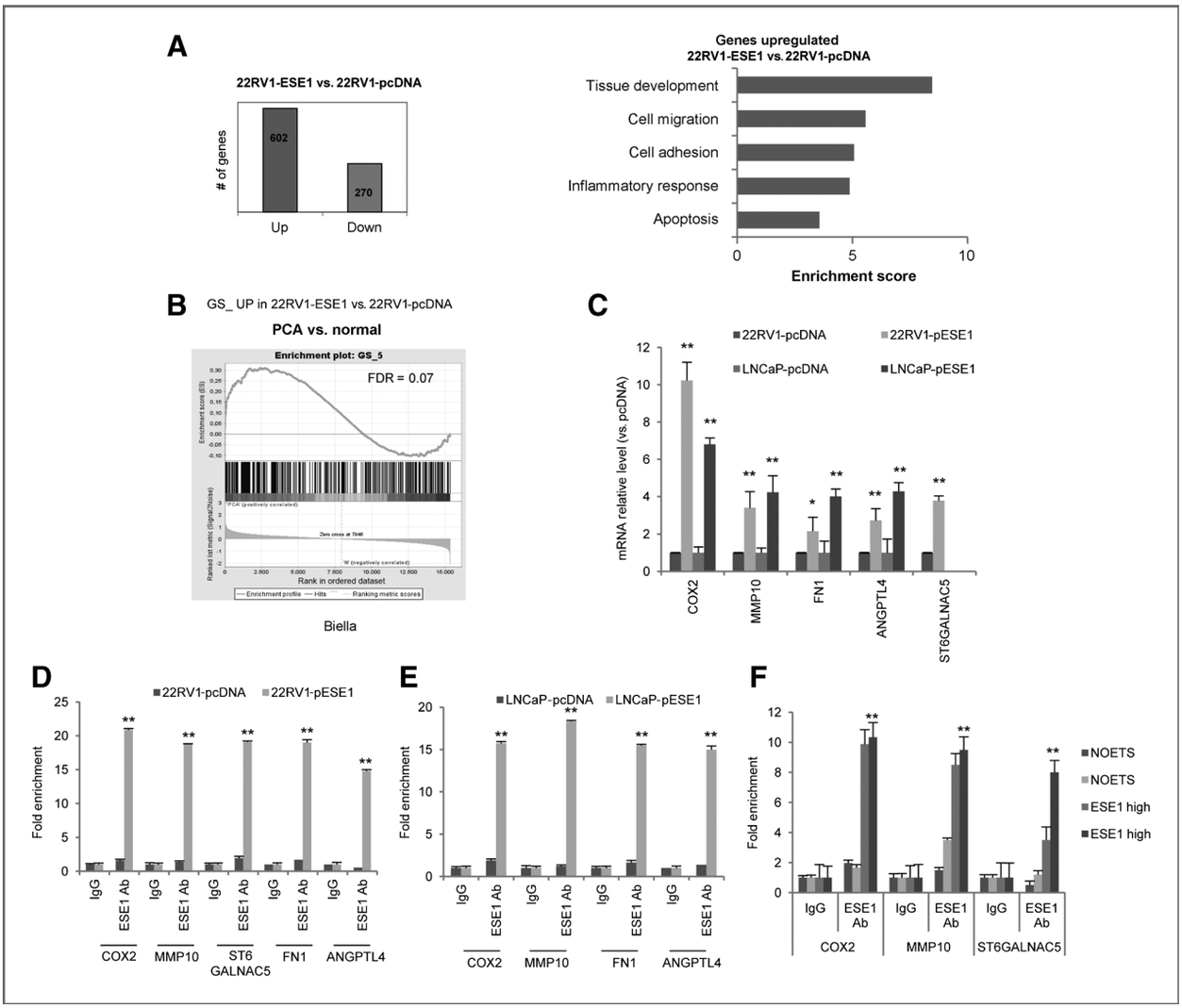

Figure 2. ESE1/ELF3 activates a transcriptional and functional program promoting inflammation and metastatic spread. A, left, number of up- and downregulated genes in 22RV1-pESE1 versus 22RV1-pcDNA cells determined by microarray analysis. Right, functional annotation of the genes significantly upregulated ($P < 0.01$) by DAVID. B, GSEA using genes upregulated in 22RV1-pESE1 comparing prostate tumors (PCa) with normal prostate in the Biella dataset. C, expression of selected genes in control (pcDNA) and ESE1/ELF3–overexpressing (pESE1) 22RV1 and LNCaP cells by qRT-PCR. D and E, binding of ESE1/ELF3 to the promoters of the indicated genes determined by chromatin immunoprecipitation and qRT-PCR in control (pcDNA) and ESE1/ELF3–overexpressing (pESE1) 22RV1 and LNCaP cells. F, binding of ESE1/ELF3 to the indicated gene promoters in prostate tumors with high ($ESE1^{high}$) or low (NOETS) expression of ESE1/ELF3. Ab, antibody; FDR, false discovery rate; IgG, immunoglobulin G. *P* values were determined using *t* test. *, $P < 0.01$; **, $P < 0.005$.

tumorigenesis. To further support the link between ESE1/ELF3 and the genes upregulated in 22RV1-pESE1, we used bioinformatics tools to identify the potential transcription factors that regulated these genes. Using ChEA, we found that the upregulated genes were highly enriched for binding of ETS transcription factors with more than 50% of genes showing promoter occupancy by one or more ETS factors ($P < 0.05$). Similarly, analysis of transcription factor interactome with MetaCore confirmed that ETS factors were among the most represented transcription factors associated with the genes induced in 22RV1-pESE1 ($P < 0.001$). Consistently, network interaction analysis using Ariadne Pathway Studio software showed that a significant number of ESE1/ELF3–induced genes were targets of ETS transcription factors (Supplementary Fig. S4). Collectively, these data implied that ESE1/ELF3 could directly regulate transcription of the induced genes.

These findings indicated that ESE1/ELF3 could contribute directly to an inflammatory gene signature in prostate tumors. The induction of genes known to be involved in inflammation, invasion, and metastasis (27) by ESE1/ELF3 in prostate cancer cells was confirmed by qRT-PCR. Expression of *COX2*, *FN1*, *MMP-10*, *ANGPTL4*, and *ST6GALNAC5* was significantly higher in ESE1/ELF3–overexpressing 22RV1 and LNCaP cells compared with control cells (Fig. 2C). Furthermore, ESE1/ELF3 was bound to the promoter of *COX2* and *MMP10*, at the level of known ETS target sites (28–30), in 22RV1-pESE1 and

LNCaP-pESE1 cells (Fig. 2D and E). We found also that ESE1/ELF3 occupied the promoters of *ST6GALNAC5*, *FN1*, and *ANGPTL4* in regions containing novel candidate ETS-binding sites (EBS) that we identified by computational analysis (Fig. 2D and E and Supplementary Fig. S5). ESE1/ELF3 occupancy of the *COX2*, *MMP10*, and *ST6GALNAC6* promoters was shown also in tissue samples of human primary prostate tumors expressing ESE1/ELF3, whereas no binding was observed in tumors with low ESE1/ELF3 expression (Fig. 2F), confirming the relevance of ESE1/ELF3 for transcriptional regulation of these genes in clinical samples.

ESE1/ELF3 is induced by IL-1β and mediates its effects in prostate cancer cells

We investigated the mechanism leading to ESE1/ELF3 overexpression in prostate tumors. Although relevant, gene amplification is likely to account only for a limited number of cases of ESE1/ELF3 overexpression. Other mechanisms leading to ESE1/ELF3 induction would be likely in place in the majority of prostate tumors. Because of the link between ESE1/ELF3 and inflammatory signaling, we hypothesized that ESE1/ELF3 could be the target of proinflammatory cytokines, such as IL-1β and could mediate its effects in prostate epithelial cells. IL-1β is frequently induced in inflammatory processes and is known to have protumorigenic effects (15, 19, 31). ESE1/ELF3 was previously shown to be induced by IL-1β in other epithelial and nonepithelial cell types (28, 29, 32, 33). However, whether ESE1/ELF3 was induced in prostate epithelial cells and could have a role in mediating the effects of IL-1β was not investigated. To verify experimentally the link between IL-1β and ESE1/ELF3, we exposed 22RV1, LNCaP, and immortalized prostate epithelial (LHS) cells to IL-1β. Treatment with IL-1β increased ESE1/ELF3 mRNA and protein level in all three cell lines (Fig. 3A and B). Interestingly, in 22RV1 cells ESE1/ELF3 mRNA increased already after 4 hours of incubation with IL-1β and remained elevated compared with unstimulated cells after 24 and 48 hours (Fig. 3C). Concomitant with the induction of ESE1/ELF3, expression of COX2, MMP10, and ST6GALNAC6 was also increased (Fig. 3C). Consistently, IL-1β treatment of 22RV1 cells induced binding of ESE1/ELF3 to the promoters of these genes (Fig. 3D). To fully assess the contribution of ESE1/ELF3 to the response to IL-1β, we knocked down ESE1/ELF3 before IL-1β induction. The level of ESE1/ELF3 was monitored at the mRNA and protein level (Fig. 3E, top and bottom). Notably, the transcriptional induction of selected target genes in response to IL-1β was prevented by ESE1/ELF3 knockdown in 22RV1 (Fig. 3E). In addition, incubation with IL-1β enhanced migration and anoikis resistance of 22RV1 prostate cancer cells and knockdown of ESE1/ELF3 reduced these effects of IL-1β (Fig. 3F and G). Together, these results showed that the transcriptional and phenotypic response of prostate cancer cells to IL-1β depended on ESE1/ELF3 and mimicked the effects of ESE1/ELF3 overexpression.

Consistent with our findings in prostate epithelial cells, we found, by analyzing the gene expression data of chondrocytes stimulated with IL-1β (34), that ESE1/ELF3 was one of the top genes induced by IL-1β in these cells ($P < 0.001$). Similarly, we found that ESE1/ELF3 was among the genes significantly upregulated ($P < 0.01$) in a IL-1β transgenic mouse model of Barrett's esophagus and esophageal carcinoma (35). To assess the contribution of ESE1/ELF3 to the IL-1β transcriptional signature in these experimental systems, we looked at the overlap with the ESE1/ELF3 gene signature in 22RV1-pESE1 cells. We observed a significant overlap between genes induced in 22RV1-pESE1 cells and in IL-1β–stimulated chondrocytes ($P = 6.414e-08$; OR, 1.8; Fig. 3H). More relevant to the cancer context, there was significant convergence between the transcriptional signature in 22RV1-pESE1 cells and genes induced in preneoplastic and neoplastic esophageal lesions in the IL-1β transgenic mice ($P < 0.0001$; Fig. 3I; Supplementary Fig. S6). In all these experimental models, the shared features were associated with relevant oncogenic pathways, particularly those associated with activation of inflammatory trascriptome such as apoptosis, migration, angiogenesis, and stress response. Furthermore, ChEA indicated that more than 40% of the shared genes showed significant occupancy by ETS factors ($P < 0.05$), and therefore could be direct targets of ESE1/ELF3. Thus, ESE1/ELF3 is induced in several models of inflammation and cancer and could contribute to the activation of inflammatory and oncogenic pathways in many preneoplastic and neoplastic conditions.

ESE1/ELF3 is required for NF-κB activation in prostate cancer cells and tumors

IL-1β induces transcription by activating NF-κB (14, 16, 36). NF-κB consists of 5 REL-related proteins and the prototypical NF-κB complex is a heterodimer of p65/RELA and p50/NFKB1 (37, 38). Proinflammatory cytokines, such as IL-1β, induce nuclear translocation of the p65 and p50 and transcriptional activation of multiple target genes (38). The ESE1/ELF3 promoter contains NF-κB–binding sites (33). Consistently, we found that IL-1β induced binding of p65 to the ESE1/ELF3 promoter, indicating that its activation occurred through NF-κB (Fig. 4A). On the other hand, the significant reversion of the transcriptional and phenotypic effects of IL-1β by ESE1/ELF3 knockdown led us to hypothesize an active role of ESE1/ELF3 in the transcriptional response to IL-1β and activation of NF-κB. Consistent with this hypothesis, we found that the activity of a NF-κB–responsive reporter was increased by IL-1β and was reduced after knockdown of ESE1/ELF3 in IL-1β–treated 22RV1 and LNCaP cells (Fig. 4B). Activity of the NF-κB reporter was also higher in stable ESE1/ELF3–overexpressing cells than in control cells, indicating that ESE1/ELF3 contributed to NF-κB activity also independently of exogenous IL-1β (Fig. 4C). Consistently, ESE1/ELF3 knockdown reduced NF-κB reporter activity in ESE1/ELF3–overexpressing LNCaP and 22RV1 cells. Interestingly, treatment with IL-1β further increased NF-κB reporter activity in ESE1/ELF3–overexpressing cells compared with IL-1β and ESE1/ELF3 overexpression alone, suggesting that ESE1/ELF3 led to increased responsiveness to IL-1β along with sustained activation of NF-κB (Fig. 4D). This was associated with further increase in ESE1/ELF3 protein levels as indicated by Western blotting, consistent with the induction of a positive feedback loop by IL-1β also in ESE1/ELF3–overexpressing cells. Next, to examine directly the contribution of ESE1/ELF3 to NF-κB

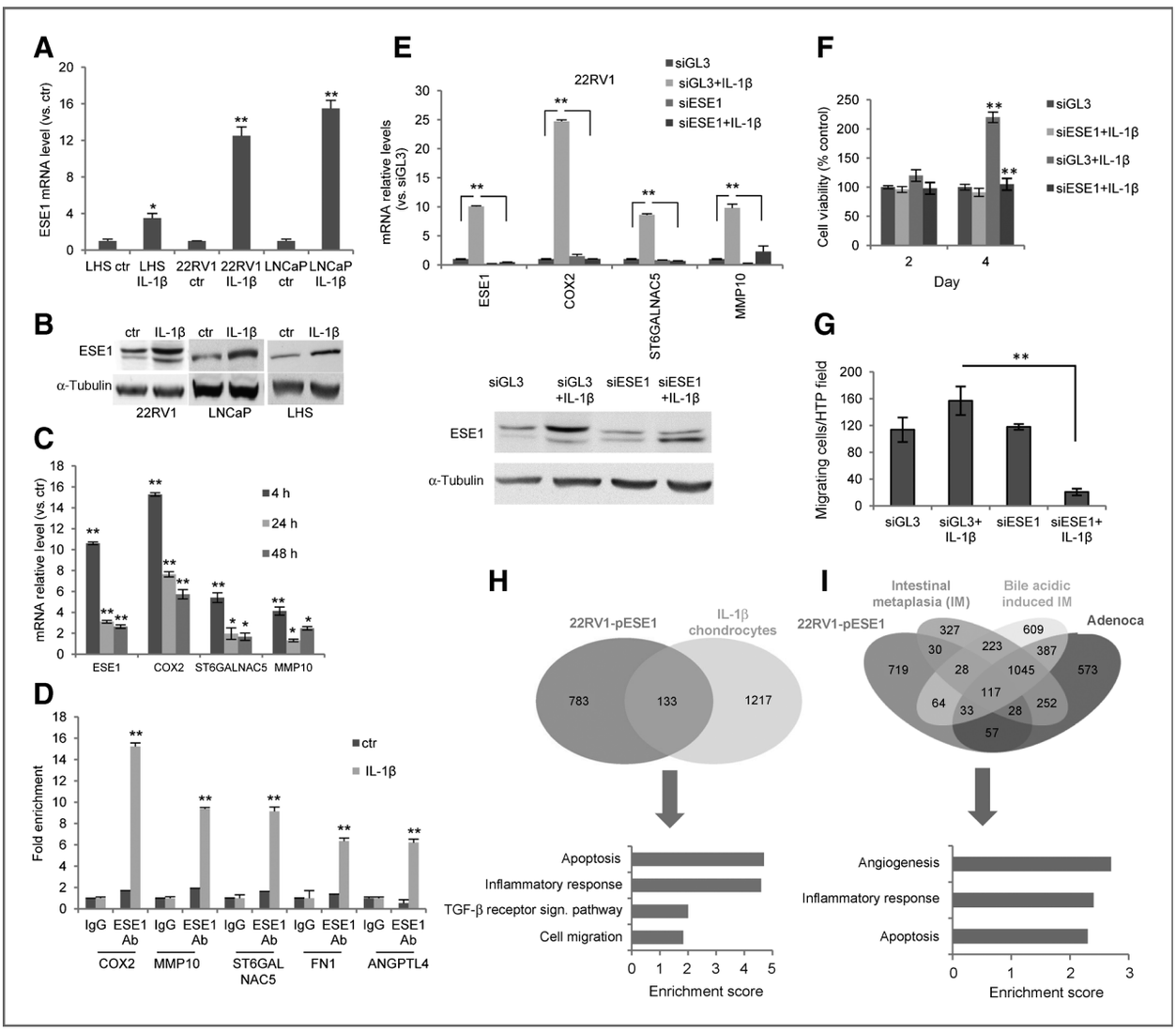

Figure 3. ESE1/ELF3 is induced by IL-1β and mediates the transforming effects of IL-1β. A, cells were exposed to IL-1β for 4 hours and ESE1/ELF3 mRNA was evaluated by qRT-PCR. B, cells were exposed to IL-1β as above and ESE1/ELF3 level determined by Western blot analysis. C, expression of ESE1/ELF3 and selected target genes determined by qRT-PCR in 22RV1 cells incubated with IL-1β for 4 hours and analyzed at the indicated time points. D, binding of ESE1/ELF3 to the promoters of the indicated genes following 4-hour treatment with IL-1β. E, top, expression of ESE1/ELF3 and the indicated target genes determined by qRT-PCR in 22RV1 cells transfected with control (siGL3) or ESE1/ELF3–targeting (siESE1) siRNA and exposed to IL-1β for 4 hours. Bottom, protein level of ESE1/ELF3 evaluated by Western blot analysis in the indicated experimental conditions. F, survival in anoikis of 22RV1 cells transfected with control (siGL3) or ESE1/ELF3–targeting (siESE1) siRNA and exposed to IL-1β for 4 hours. G, Boyden chamber assay with 22RV1 cells transfected with control (siGL3) or ESE1/ELF3–targeting (siESE1) siRNA and exposed for 4 hours to IL-1β. H, Venn diagram showing the overlap between genes upregulated in ESE1/ELF3–overexpressing 22RV1 cells and genes induced by IL-1β in chondrocytes (top) and functional annotation of the common genes (bottom). I, Venn diagram showing the overlap between genes upregulated in ESE1/ELF3 overexpressing 22RV1 cells and prenoplastic (intestinal metaplasia and bile acidic metaplasia) and esophageal adenocarcinoma lesions in the IL-1β transgenic mice (top) and functional annotation of the genes in common (bottom). *P* values were determined using *t* test. *, $P < 0.01$; **, $P < 0.005$. All data are mean ± SEM. Ab, antibody; IgG, immunoglobulin G.

transcriptional activity, we assessed the binding of p65 to COX2 and IL-6 promoters, two known NF-κB targets (29, 33, 39). We determined that expression of COX2 increased both in IL-1β–treated cells and in ESE1/ELF3–overexpressing cells. We found that IL-1β induced and knockdown of ESE1/ELF3 prevented binding of p65 to the COX2 promoter (Fig. 4E). Similar to COX2, IL-6 promoter occupancy by p65 (Fig. 4E) and IL-6 mRNA (Fig. 4F) were induced by IL-1β and both effects were blocked by ESE1/ELF3 knockdown. These data established for the first time the notion that ESE1/ELF3 actively contributes to NF-κB activation by enhancing binding of NF-κB to target gene promoters.

Bioinformatic analyses further supported a direct contribution of ESE1/ELF3 in the activation of NF-κB target genes. Transcription factors interactome analysis with MetaCore showed that genes induced by ESE1/ELF3 in 22RV1 cells

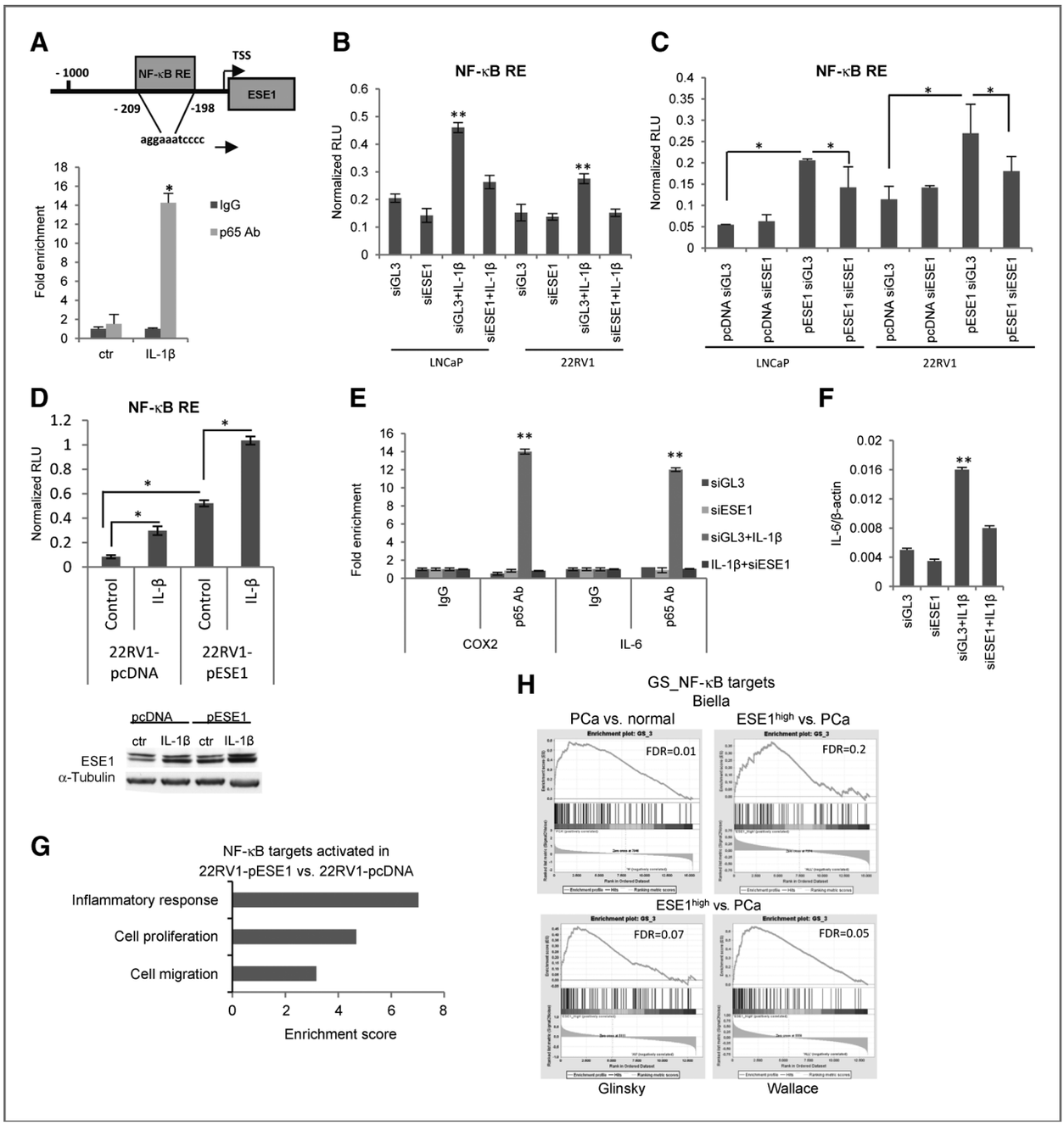

Figure 4. ESE1/ELF3 promotes NF-κB activation. A, top, ESE1/ELF3 promoter region and position of the NF-κB–binding site (NF-κB RE). Bottom, binding of p65 to ESE1/ELF3 promoter after IL-1β treatment in 22RV1 cells. B, NF-κB reporter activity following IL-1β treatment and ESE1/ELF3 downregulation in LNCaP and 22RV1 cells. RLU, relative luciferase light unit. C, NF-κB reporter activity in control (pcDNA) and ESE1/ELF3–overexpressing (pESE1) cells following ESE1/ELF3 downregulation. D, NF-κB reporter activity in control (pcDNA) and ESE1/ELF3–overexpressing (pESE1) 22RV1 cells after 4-hour exposure to IL-1β. Bottom, level of ESE1/ELF3 assessed by Western blot analysis in 22RV1-pcDNA and 22RV1-pESE1 following IL-1β treatment. E, p65 binding to the COX2 and IL-6 promoter in 22RV1 cells transfected with control (siGL3) or ESE1/ELF3–targeting (siESE1) siRNA and exposed to IL-1β for 4 hours. F, IL-6 mRNA determined by qRT-PCR in 22RV1 cells transfected with control (siGL3) or ESE1/ELF3 targeting (siESE1) siRNA and exposed to IL-1β for 4 hours. *P* values were determined using *t* test. G, functional annotation analysis by DAVID of NF-κB targets activated in 22RV1-pESE1 cells. H, GSEA using gene sets of NF-κB–regulated genes comparing prostate tumors with normal prostate samples in the Biella microarray dataset and ESE1^{high} with all the other tumors (ESE1^{high} vs. PCa) in the indicated microarray datasets *, $P < 0.01$; **, $P < 0.005$. All data are mean ± SEM. Ab, antibody; FDR, false discovery rate.

were significantly enriched for targets of p65 ($P = 4.4990E{-}06$) and p50 ($P = 0.007$). Notably, NF-κB target genes induced by ESE1/ELF3 were preferentially related to cell proliferation, migration, and inflammation (Fig. 4G). A significant enrichment of p65 targets was also found among the genes induced in ESE1/ELF3–overexpressing 22RV1 cells and shared with

IL-1β–stimulated chondrocytes ($P = 1.9690E-11$), and preneoplastic and neoplastic esophageal lesions in IL-1β transgenic mice ($P = 3.0E-05$). Ariadne pathway analysis revealed the existence of reciprocal regulatory loops between ESE1/ELF3- and NF-κB–regulated genes (Supplementary Fig. S7). Furthermore, GSEA in prostate cancer microarray datasets revealed significant enrichment of NF-κB target genes in prostate tumors compared with normal prostate and prevalent enrichment in particular in tumors with high ESE1/ELF3 expression ($ESE1^{high}$ tumors) compared with all other tumors (Fig. 4H). Thus, the transcriptional program orchestrated by ESE1/ELF3 both in prostate cell lines and tumors involved numerous NF-κB–regulated genes. Induction of these common targets contributes to the activation of relevant oncogenic pathways as indicated by functional annotation analysis.

ESE1/ELF3 and NF-κB constitute a positive feedback loop, leading to constitutive NF-κB activation

To further define the contribution of ESE1/ELF3 to NF-κB activation, we examined the expression and intracellular localization of p50 and p65 in both stably overexpressing ESE1/ELF3 and IL-1β–stimulated 22RV1 cells. Both the level and nuclear localization of p50 and p65 were increased in ESE1/ELF3–overexpressing 22RV1 cells as revealed by immunofluorescence (Fig. 5A) and Western blot analysis (Fig. 5B). Nuclear p50 and p65 increased about 2- and more than 6-fold, respectively, as determined by densitometric analysis of the immunoblots. After IL-1β treatment of 22RV1 cells, we observed a similar increase of total and nuclear level of p50 and p65 along with ESE1/ELF3 (Supplementary Fig. S8). Notably, knockdown of ESE1/ELF3 reduced cytoplasmic and nuclear p50 and p65 in IL-1β–treated cells (Supplementary Fig. S8), indicating that ESE1/ELF3 was required for NF-κB accumulation and nuclear translocation following IL-1β stimulation. To show that ESE1/ELF3 sustained NF-κB activation also *in vivo*, we evaluated the level of p50 and p65 in tumor xenografts produced by 22RV1-pESE1 and 22RV1-pcDNA cells. There was a significant increase (>5-fold by densitometric analysis) of nuclear p50 and p65 in the 22RV1-pESE1 tumor xenografts compared with control tumors (Fig. 5C). Furthermore, several ESE1/ELF3 and NF-κB target genes were overexpressed in 22RV1-pESE1 tumor xenografts (Fig. 5D).

Interestingly, we observed that both in stable overexpressing cell lines and in IL-1β–treated cells p50 and p65 largely colocalized with ESE1/ELF3 (Fig. 5A and Supplementary Fig. S8). Therefore, we tested whether ESE1/ELF3 interacted directly with p50 and p65. Immunoprecipitation with an antibody directed to ESE1/ELF3 coimmunoprecipitated p50 and p65 in 22RV1-pESE1 cells (Fig. 5E). In addition, ESE1/ELF3 was immunoprecipitated, along with p65, by an anti-p50 antibody, confirming the physical interaction between ESE1/ELF3 and the NF-κB subunits. Through these protein–protein interactions, ESE1/ELF3 could affect stability, nuclear localization, and promoter recruitment of the NF-κB subunits. In addition, we hypothesized that ESE1/ELF3 could control NF-κB at the transcriptional level. The NFKB1 gene promoter contains EBS (Fig. 5F; 40), suggesting the possibility that ESE1/ELF3 could control p50 transcription. We found higher expression of p50 in ESE1/ELF3–overexpressing cells (Fig. 5G). Furthermore, p50 increased after stimulation of 22RV1 cells with IL-1β and its induction was reduced by ESE1/ELF3 knockdown (Fig. 5H). The level of p50 was also significantly increased in the 22RV1-pESE1 compared with the 22RV1-pcDNA tumor xenografts (Fig. 5D). Consistently, ChIP showed binding of ESE1/ELF3 to the NFKB1 promoter in the region containing the predicted EBS in ESE1/ELF3–overexpressing cells (Fig. 5I) and in IL-1β–treated 22RV1 cells (Fig. 5J). Therefore, the ability of ESE1/ELF3 to interact with the NF-κB pathway at multiple levels results in a positive feedback loop leading to sustained activation of NF-κB and induction of multiple oncogenic targets in prostate cancer cells.

ESE1/ELF3 sustains NF-κB activation in metastatic prostate cancer cells

Among the prostate cancer cell lines tested, we noticed that DU145 cells expressed a high level of ESE1/ELF3, comparable with high ESE1/ELF3–expressing human tumors (Supplementary Fig. S2D). DU145 cells are a metastatic prostate cancer cell line and several studies have shown previously that NF-κB is active in these cells (41, 42). However, the role of ESE1/ELF3 in sustaining cell transformation and NF-κB activation in these cells in DU145 is unknown. Immunofluorescence revealed that ESE1/ELF3 was highly expressed in DU145 prevalently in the nuclear compartment but also in the cytoplasm and that it colocalized with both p50 and p65 NF-κB subunits (Fig. 6A). The physical interaction between ESE1/ELF3 and the NF-κB subunits was also shown by coimmunoprecipitation (Fig. 6B). To further understand the functional role of ESE1/ELF3 in DU145 cells, we knocked down expression of the gene using 2 siRNA targeting different regions of the gene. Effective knockdown of ESE1/ELF3 was assessed at the mRNA and protein level (Fig. 6C, bottom and top left). Concomitantly, expression of several NF-κB and ESE1/ELF3 target genes was significantly reduced using both of the ESE1/ELF3 siRNAs ($P < 0.01$; Fig. 6C). Relevantly, chromatin immunoprecipitation confirmed that ESE1/ELF3 occupied the promoter of the selected target genes and ESE1/ELF3 knockdown significantly reduced the promoter occupancy (Fig. 6D). Notably, ESE1/ELF3 knockdown reduced the intranuclear levels of p65 and p50, indicating that ESE1/ELF3 facilitated nuclear accumulation of active NF-κB complexes in these cells (Fig. 6E). Consistently, we found that NF-κB reporter activity was high in DU145 cells and was significantly reduced by knocking down ESE1/ELF3 expression (Fig. 6F). Furthermore, we found that ESE1/ELF3 knockdown significantly reduced the ability to form anchorage-independent colonies, suggesting that it contributed to the transformed phenotype of DU145 cells (Fig. 6G). Collectively, these data point to a role of ESE1/ELF3 in sustaining constitutive activation of NF-κB independent of IL-1β stimulation in this metastatic prostate cancer cell line.

ESE1/ELF3 and NF-κB activation are associated with poor prognosis

To determine the clinical relevance of these findings, we assessed concomitantly the protein expression of p50, p65, and ESE1/ELF3 in TMAs of patients with prostate cancer for

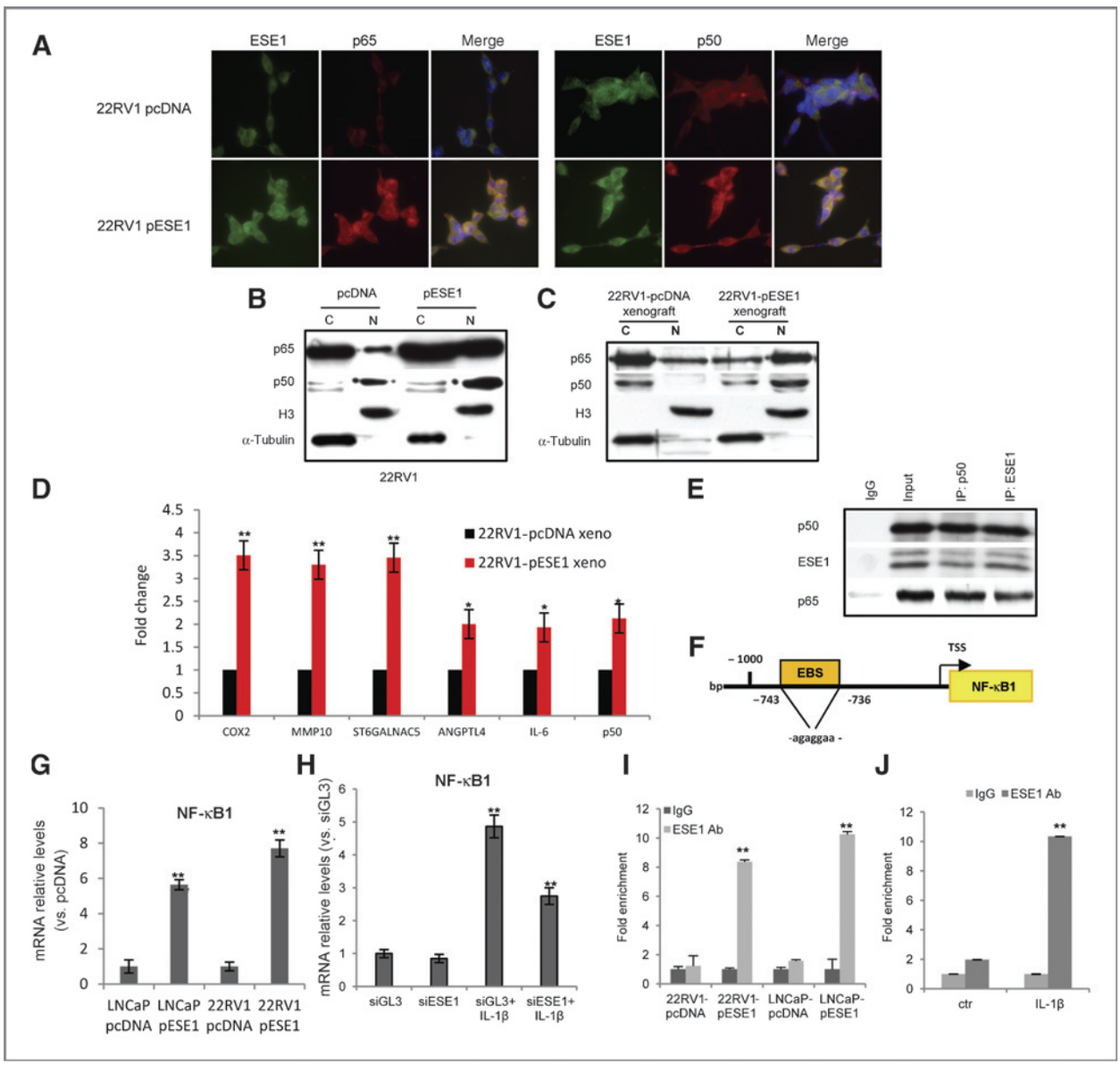

Figure 5. ESE1/ELF3 and NF-κB constitute a positive feedback loop leading to NF-κB pathway activation. A, immunofluorescence microscopy detection of ESE1/ELF3 (green), p50 (red, left), p65 (red, right), and nuclei (blue) in 22RV1-pcDNA and 22RV1-pESE1. B, level of p65 and p50 assessed by Western blot analysis in cytoplasmic (C) and nuclear (N) fractions from 22RV1-pcDNA and 22RV1-pESE1. C, level of p65 and p50 assessed by Western blot analysis in cytoplasmic (C) and nuclear (N) fractions from 22RV1-pcDNA and 22RV1-pESE1 tumor xenografts. D, expression of selected target genes determined by qRT-PCR in xenografts derived from 22RV1-pcDNA and 22RV1-pESE1. E, lysates of 22RV1-pESE1 cells were immunoprecipitated with antibodies against ESE1/ELF3 and p50 and analyzed by immunoblotting with the indicated antibodies. F, position of ESE1/ELF3–binding site (EBS) in the NFKB1 promoter. G, p50/NFKB1 mRNA in control (pcDNA) and ESE1/ELF3–overexpressing (pESE1) cells determined by qRT-PCR. H, p50/NFKB1 mRNA determined by qRT-PCR in 22RV1 cells after IL-1β exposure with and without ESE1/ELF3 knockdown. I, binding of ESE1/ELF3 to the NFKB1 promoter evaluated by ChIP in control and ESE1/ELF3 overexpressing LNCaP and 22RV1 cells. J, binding of ESE1/ELF3 to the NFKB1 promoter evaluated in control and after IL-1β exposure in 22RV1 cells. Ab, antibody; IgG, immunoglobulin G.

which we had long-term clinical follow-up data (Fig. 7A; ref. 22). We found a significant association between overexpression of ESE1/ELF3 and nuclear p50 and p65 ($P = 0.0005$; OR, 14.4). Specifically, 22% of prostate tumors exhibited strong nuclear staining for p50 and p65, with about 40% of those being positive for both (Fig. 7B). Nuclear p50 and p65 positivity was exclusively associated with ESE1/ELF3–positive tumors of ESE1/ELF3, although not all of the ESE1/ELF3–positive tumors showed nuclear p50 and p65 staining (Fig. 7C). Thus, concomitant expression of ESE1/ELF3 and nuclear p50 and p65 positivity were present in a subset of prostate tumors.

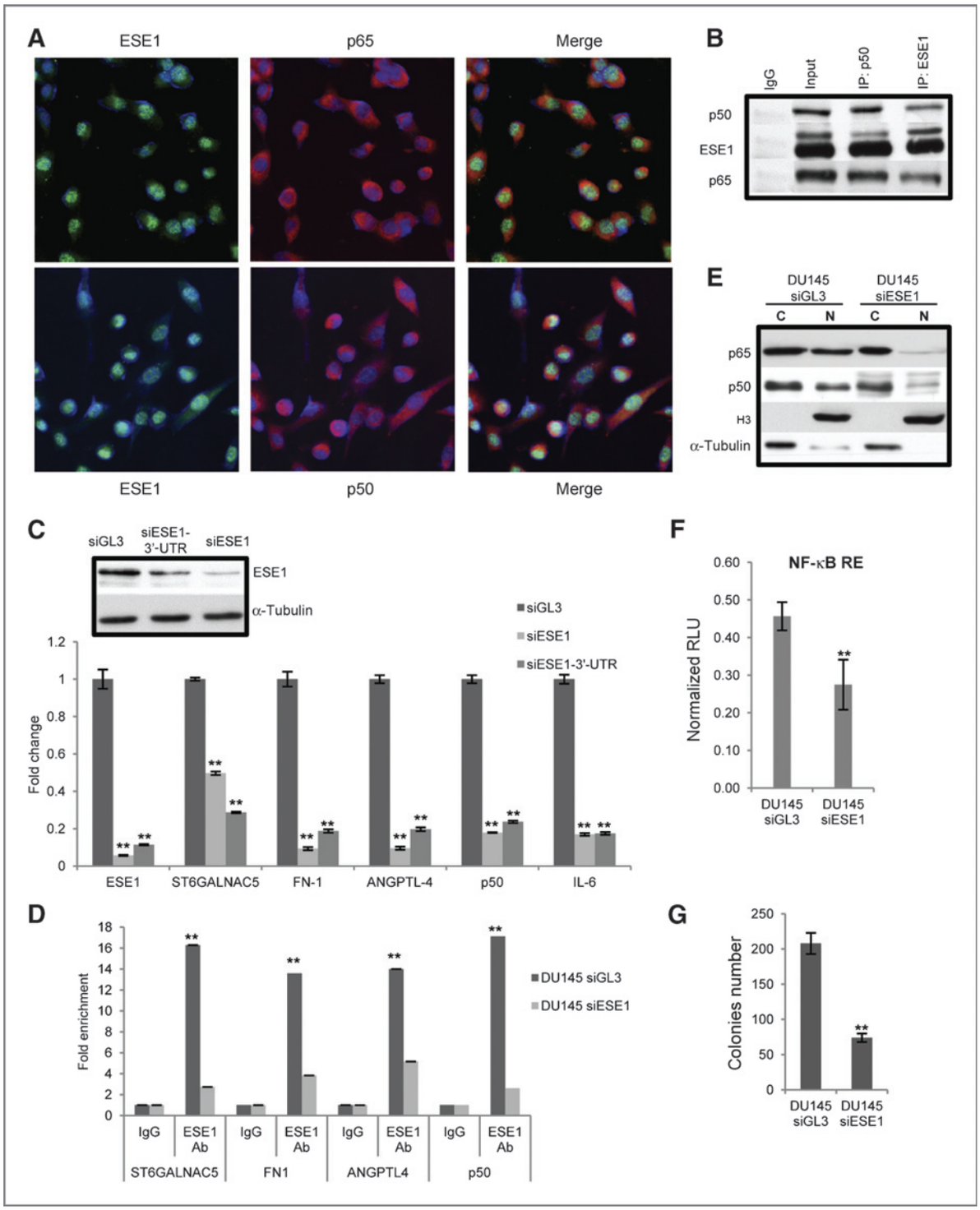

Figure 6. ESE1/ELF3 sustains transformation and NF-κB activation in metastatic prostate cancer cells. A, immunofluorescence microscopy detection of ESE1/ELF3 (green), p65 (red, top), p50 (red, bottom), and nuclei (blue) in DU145. B, lysates of DU145 cells were immunoprecipitated with antibodies against ESE1/ELF3 and p50 and analyzed by immunoblotting with the indicated antibodies. C, top, protein level of ESE1/ELF3 evaluated by Western blot analysis following ESE1/ELF3 knockdown in DU145 cells. Bottom, mRNA level of ESE1/ELF3 and selected target genes evaluated by qRT-PCR in DU145 cells following ESE1/ELF3 knockdown with 2 ESE1/ELF3 targeting siRNA (siESE1 and siESE1-3′-UTR). D, ESE1/ELF3 occupancy on selected target gene promoters evaluated by ChIP in DU145 cells transfected with control siRNA (siGL3) or with ESE1/ELF3–targeting siRNA (siESE1). E, Western blot analysis of p65 and p50 in nuclear and cytoplasmic fractions following ESE1/ELF3 knockdown in DU145 cells. F, NF-κB reporter activity following ESE1/ELF3 knockdown in DU145 cells. G, colony formation in soft agar following ESE1/ELF3 knockdown in DU145. *P* values were determined using *t* test. **, $P < 0.005$; All data are mean ± SEM; Ab, antibody; IgG, immunoglobulin G; RLU, relative luciferase light unit.

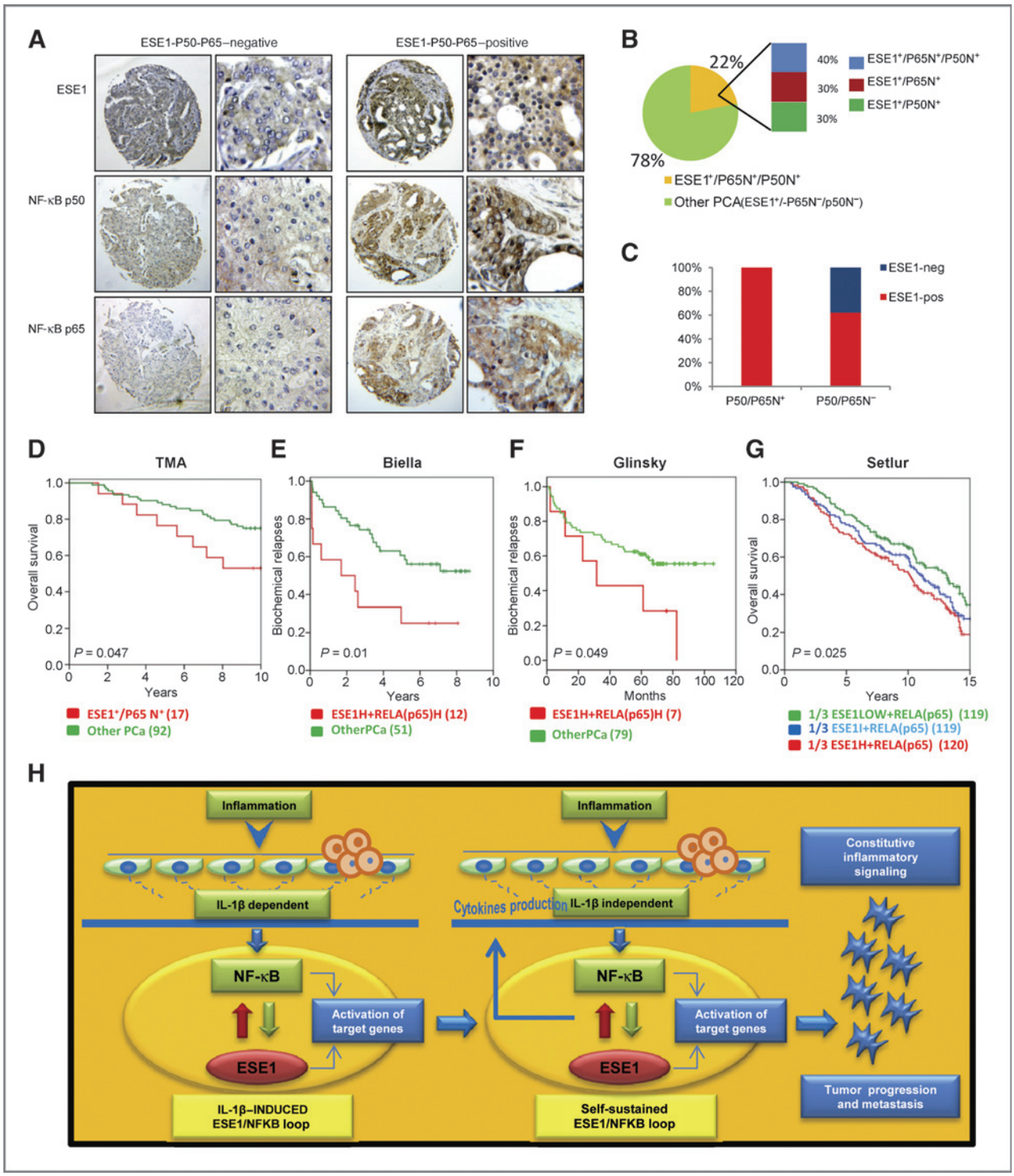

Figure 7. Expression of ESE1/ELF3 and NF-κB activation are associated with poor prognosis. A, representative images of immunohistochemical staining for ESE1/ELF3 and NF-κB subunits p50 and p65 in prostate tumors. B, distribution of ESE1/ELF3, nuclear p65, and p50 staining in prostate tumors ($n = 186$). N^+, positive nuclear stain. C, percentage of ESE1/ELF3-positive and -negative tumors according to nuclear p50 and p65 staining evaluated by IHC as described earlier. D, Kaplan–Meier analysis of overall survival of the patients cohort analyzed by TMA divided according to ELF3/ESE1 and nuclear p65 staining. E and F, Kaplan–Meier analysis of biochemical relapse-free survival of patients in the Biella and Glinsky cohort analyzed by microarrays divided according to ELF3/ESE1 and p65/RELA mRNA level. G, Kaplan–Meier analysis of overall survival of patients in the Setlur cohort divided according to ESE1/ELF3 and p65/RELA mRNA level. *P* values determined by log-rank test (Mantel–Cox). Number of patients is indicated in parenthesis. H, proposed model for the induction of ESE1/ELF3 by IL-1β and establishment of a positive feedback loop leading to constitutive activation of NF-κB and inflammatory signaling in prostate tumors.

On the basis of our biologic and genomic data, we hypothesized that these features could mark particularly clinically aggressive tumors. Consistent with this hypothesis, we found that high expression of ESE1/ELF3 and nuclear p65 positivity (43–45) were significantly associated with shorter survival of patients after prostatectomy ($P = 0.047$; Fig. 7D). Furthermore, high ESE1/ELF3 and p65/RELA mRNA expression in patient cohorts examined by microarrays (5) was associated with increased biochemical relapses after prostatectomy ($P = 0.01$; Fig. 7E and F). A similar trend was observed when we considered the protein level of ESE1/ELF3 and nuclear positivity for both p50 and p65 determined by IHC in TMAs ($P = 0.06$; Supplementary Fig. S9A) and high mRNA level of ESE1/ELF3, p65/RELA, and p50/NFKB1 in microarray data ($P = 0.038$; Supplementary Fig. S9B). Relevantly, we found that the combined upregulation of ESE1/ELF3 and p65/RELA mRNA was also significantly associated with reduced overall survival after prostatectomy ($P = 0.025$) in an independent gene expression study of patients with prostate cancer with 15-year clinical follow-up (Fig. 7G; ref. 46). Together, these findings showed the prognostic value of combined ESE1/ELF3 upregulation and NF-κB activation in prostate tumors and further reinforced the notion of their relevance for prostate cancer progression.

Discussion

This study establishes for the first time that the ETS factor ESE1/ELF3 has an oncogenic activity and a crucial role in constitutive and cytokine-induced activation of NF-κB in prostate tumors. Here, we report a novel mechanism leading to activation of a oncogenic ETS transcription factor, independent of chromosomal translocation, and linking inflammation, NF-κB activation, and prostate cancer progression. We show that ESE1/ELF3 is a key element in a positive feedback loop involving the proinflammatory cytokine IL-1β and the NF-κB subunits p50 and p65, and that ESE1/ELF3 expression is instrumental for the proinflammatory and protumorigenic functions of this pathway. Chronic inflammation is an important risk factor for prostate cancer and involves the production of multiple cytokines in response to several inflammatory stimuli (13, 19). IL-1β is one of the major cytokines implicated in inflammation in the prostate (15). NF-κB has been reported to contribute to increased proliferation, survival, angiogenesis, and metastatic progression in prostate cancer and activation of the NF-κB pathway is associated with aggressive clinical behavior (44, 45). We found that ESE1/ELF3 is frequently overexpressed in human primary and metastatic prostate cancers. ESE1/ELF3 is also amplified in a small but relevant number of cases. Consistent with an oncogenic role, we show that ESE1/ELF3 controls a network of genes involved in cell invasion, migration, inflammation, and metastasis, and its overexpression enhances the transformed properties of prostate cancer cells and promotes tumor growth and metastasis in mouse xenografts. We found that IL-1β induces ESE1/ELF3 in prostate epithelial cells through activation of NF-κB and binding of p65 to the ESE1/ELF3 promoter. In turn, ESE1/ELF3 contributes to the activation of NF-κB by transcriptional regulation of p50 and posttranscriptional control of both p50 and p65 function. We show that ESE1/ELF3 interacts with both p50 and p65 proteins and enhances their nuclear translocation and binding to target gene promoters. Relevantly, we found that ESE1/ELF3 contributed to NF-κB activation also in the absence of cytokine stimulation and that this effect was maintained *in vivo* in tumor xenografts of ESE1/ELF3–overexpressing cells. ESE1/ELF3 sustained constitutive NF-κB activation also in metastatic prostate cancer DU145 cells expressing endogenously high levels of ESE1/ELF3. This suggests that, once a significant level of induction of ESE1/ELF3 is reached, activation of the pathway could be self-sustained in the absence of external inflammatory stimuli. In addition, production of cytokines such as IL-6 by prostate cancer cells in response to ESE1/ELF3 and NF-κB activation could contribute in an autocrine (cell-autonomous) way to the positive feedback loop and inflammatory signaling. On the basis of these multiple lines of evidence, we propose that the reciprocal interactions between ESE1/ELF3 and NF-κB result in sustained activation of NF-κB, greater responsiveness to proinflammatory stimuli, and activation of combined ESE1/ELF3 and NF-κB target genes that accelerate prostate cancer progression (Fig. 7H). Consistently, we found that the level of ESE1/ELF3 was significantly higher in metastatic tumors compared with primary prostate tumors suggesting that the gene plays a role in tumor progression.

Bioinformatics analyses and functional studies further support the link between ESE1/ELF3, IL-1β, and NF-κB and their involvement in tumor progression. Notably, we found a significant convergence between the transcriptional program observed in ESE1/ELF3–overexpressing prostate cancer cells and IL-1β–induced transcriptional signatures in experimental models of inflammatory, preneoplastic, and neoplastic diseases. Intriguingly, this convergence was observed in IL-1β transgenic mouse model of Barrett's esophagus (35), an established preneoplastic condition functionally related to chronic inflammation and IL-1β, suggesting that the ESE1/ELF3–NF-κB axis could be relevant also in other types of cancers. Moreover, both in human cell lines and prostate tumors, we observed a convergence of ESE1/ELF3- and NF-κB–regulated genes. This finding was also supported by the enrichment of NF-κB target genes by GSEA in human prostate tumors with high expression of ESE1/ELF3. Moreover, analysis of large sets of clinical samples provided evidence that this positive feedback loop operates in a subset of prostate cancers and could drive disease recurrence and progression to metastatic lethal disease. About 25% of primary tumors showed increased expression of ESE1/ELF3 and nuclear p65 by IHC. Notably, high levels of ESE1/ELF3 and nuclear p65 positivity were associated with shorter overall survival after prostatectomy. Similarly, high levels of ESE1/ELF3 and p65 mRNA, with and without p50, in microarray datasets were associated with increased biochemical relapse and shorter overall survival. These findings call for assessment of ESE1/ELF3 and p65/RELA as potential prognostic biomarkers in prostate cancer. Furthermore, their evaluation in clinical samples could guide the implementation of targeted treatment strategies for patients with

prostate cancer. In addition to uncovering a mechanistic link between ESE1/ELF3 and NF-κB in prostate tumorigenesis, this study opens avenues for patient risk stratification and indicates a rationale for context-dependent therapeutic approaches in specific subsets of patients with prostate cancer. The role of ESE1/ELF3 and its association with NF-κB activation in patients with clinically localized but aggressive and high-risk prostate tumors point to the possibility that targeting the NF-κB pathway with inhibitors that are currently in preclinical and clinical development (47) could be a valid therapeutic strategy.

Disclosure of Potential Conflicts of Interest

No potential conflicts of interest were disclosed.

Authors' Contributions

Conception and design: N. Longoni, C.V. Catapano, G.M. Carbone
Development of methodology: N. Longoni, M. Sarti, D. Albino, A. Malek, G. Chiorino, C.V. Catapano, G.M. Carbone
Acquisition of data (provided animals, acquired and managed patients, provided facilities, etc.): N. Longoni, D. Albino, G. Civenni, A. Malek, E. Ortelli, S. Pinton, G. D'Ambrosio, F. Sessa, G.N. Thalmann, G.M. Carbone
Analysis and interpretation of data (e.g., statistical analysis, biostatistics, computational analysis): N. Longoni, M. Sarti, A. Malek, M. Mello-Grand, P. Ostano, R. Garcia-Escudero, G.N. Thalmann, G. Chiorino, G.M. Carbone
Writing, review, and/or revision of the manuscript: G.N. Thalmann, C.V. Catapano, G.M. Carbone
Administrative, technical, or material support (i.e., reporting or organizing data, constructing databases): D. Albino, S. Pinton, G.N. Thalmann, G.M. Carbone
Study supervision: C.V. Catapano, G.M. Carbone
Other: Pathological study (Grading and Staging of prostatic cancer), F. Sessa; Immunohistochemistry, F. Sessa

Acknowledgments

The authors thank Dr. Towia Libermann for the gift of the pESE1/ELF3 expressing vector.

Grant Support

This work was supported by grants from Oncosuisse (KFS-01913-08 and KFS-02573-02-2010), Swiss National Science Foundation (FNS-31003A-118113), Ticino Foundation for Cancer Research, Fondazione Virginia Boeger and Fondazione Fidinam (G.M. Carbone and C.V. Catapano). M. Mello-Grand and G. Chiorino were supported by Compagnia di San Paolo, Torino, Italy, and AIRC, Associazione Italiana per la Ricerca sul Cancro (MFAG-11742). R. Garcia-Escudero was supported by an SNSF International Short Visit Fellowship.

The costs of publication of this article were defrayed in part by the payment of page charges. This article must therefore be hereby marked *advertisement* in accordance with 18 U.S.C. Section 1734 solely to indicate this fact.

Received December 14, 2012; revised April 23, 2013; accepted May 7, 2013; published OnlineFirst May 16, 2013.

References

1. Jemal A, Bray F, Center MM, Ferlay J, Ward E, Forman D. Global cancer statistics. CA Cancer J Clin 2011;61:69–90.
2. Rubin MA, Maher CA, Chinnaiyan AM. Common gene rearrangements in prostate cancer. J Clin Oncol 2011;29:3659–68.
3. Clark JP, Cooper CS. ETS gene fusions in prostate cancer. Nat Rev Urol 2009;6:429–39.
4. Tomlins SA, Rhodes DR, Perner S, Dhanasekaran SM, Mehra R, Sun XW, et al. Recurrent fusion of TMPRSS2 and ETS transcription factor genes in prostate cancer. Science 2005;310:644–8.
5. Kunderfranco P, Mello-Grand M, Cangemi R, Pellini S, Mensah A, Albertini V, et al. ETS transcription factors control transcription of EZH2 and epigenetic silencing of the tumor suppressor gene Nkx3.1 in prostate cancer. PLoS ONE 2010;5:e10547.
6. Cangemi R, Mensah A, Albertini V, Jain A, Mello-Grand M, Chiorino G, et al. Reduced expression and tumor suppressor function of the ETS transcription factor ESE-3 in prostate cancer. Oncogene 2008;27:2877–85.
7. Albino D, Longoni N, Curti L, Mello-Grand M, Pinton S, Civenni G, et al. ESE3/EHF controls epithelial cell differentiation and its loss leads to prostate tumors with mesenchymal and stem-like features. Cancer Res 2012;72:2889–900.
8. Vitari AC, Leong KG, Newton K, Yee C, O'Rourke K, Liu J, et al. COP1 is a tumour suppressor that causes degradation of ETS transcription factors. Nature 2011;474:403–6.
9. Chi P, Chen Y, Zhang L, Guo X, Wongvipat J, Shamu T, et al. ETV1 is a lineage survival factor that cooperates with KIT in gastrointestinal stromal tumours. Nature 2010;467:849–53.
10. Oettgen P, Alani RM, Barcinski MA, Brown L, Akbarali Y, Boltax J, et al. Isolation and characterization of a novel epithelium-specific transcription factor, ESE-1, a member of the ets family. Mol Cell Biol 1997;17:4419–33.
11. Oliver JR, Kushwah R, Hu J. Multiple roles of the epithelium-specific ETS transcription factor, ESE-1, in development and disease. Lab Invest 2012;92:320–30.
12. Seth A, Watson DK. ETS transcription factors and their emerging roles in human cancer. Eur J Cancer 2005;41:2462–78.
13. De Marzo AM, Platz EA, Sutcliffe S, Xu J, Grönberg H, Drake CG, et al. Inflammation in prostate carcinogenesis. Nat Rev Cancer 2007;7:256–69.
14. Perkins ND. The diverse and complex roles of NF-kappaB subunits in cancer. Nat Rev Cancer 2012;12:121–32.
15. Jerde TJ, Bushman W. IL-1 induces IGF-dependent epithelial proliferation in prostate development and reactive hyperplasia. Sci Signal 2009;2:ra49.
16. Sims JE, Smith DE. The IL-1 family: regulators of immunity. Nat Rev Immunol 2010;10:89–102.
17. Karin M. Nuclear factor-kappaB in cancer development and progression. Nature 2006;441:431–6.
18. Ben-Neriah Y, Karin M. Inflammation meets cancer, with NF-kappaB as the matchmaker. Nat Immunol 2011;12:715–23.
19. Zitvogel L, Kepp O, Galluzzi L, Kroemer G. Inflammasomes in carcinogenesis and anticancer immune responses. Nat Immunol 2012;13:343–51.
20. Longoni N, Kunderfranco P, Pellini S, Albino D, Mello-Grand M, Pinton S, et al. Aberrant expression of the neuronal-specific protein DCDC2 promotes malignant phenotypes and is associated with prostate cancer progression. Oncogene 2013;32:2315–24.
21. Malek A, Núñez LE, Magistri M, Brambilla L, Jovic S, Carbone GM, et al. Modulation of the activity of Sp transcription factors by mithramycin analogues as a new strategy for treatment of metastatic prostate cancer. PLoS ONE 2012;7:e35130.
22. Prtilo A, Leach FS, Markwalder R, Kappeler A, Burkhard FC, Cecchini MG, et al. Tissue microarray analysis of hMSH2 expression predicts outcome in men with prostate cancer. J Urol 2005;174:1814–8.
23. Glinsky GV, Glinskii AB, Stephenson AJ, Hoffman RM, Gerald WL. Gene expression profiling predicts clinical outcome of prostate cancer. J Clin Invest 2004;113:913–23.
24. Wallace TA, Prueitt RL, Yi M, Howe TM, Gillespie JW, Yfantis HG, et al. Tumor immunobiological differences in prostate cancer between African-American and European-American men. Cancer Res 2008;68:927–36.
25. Tomlins SA, Laxman B, Dhanasekaran SM, Helgeson BE, Cao X, Morris DS, et al. Distinct classes of chromosomal rearrangements create oncogenic ETS gene fusions in prostate cancer. Nature 2007;448:595–9.
26. Ateeq B, Tomlins SA, Laxman B, Asangani IA, Cao Q, Cao X, et al. Therapeutic targeting of SPINK1-positive prostate cancer. Sci Transl Med 2011;3:72ra17.

27. Nguyen DX, Bos PD, Massagué J. Metastasis: from dissemination to organ-specific colonization. Nat Rev Cancer 2009;9:274–84.
28. Grall F, Gu X, Tan L, Cho JY, Inan MS, Pettit AR, et al. Responses to the proinflammatory cytokines interleukin-1 and tumor necrosis factor alpha in cells derived from rheumatoid synovium and other joint tissues involve nuclear factor kappaB-mediated induction of the Ets transcription factor ESE-1. Arthritis Rheum 2003;48:1249–60.
29. Grall FT, Prall WC, Wei W, Gu X, Cho JY, Choy BK, et al. The Ets transcription factor ESE-1 mediates induction of the COX-2 gene by LPS in monocytes. FEBS J 2005;272:1676–87.
30. Heo SH, Choi YJ, Ryoo HM, Cho JY. Expression profiling of ETS and MMP factors in VEGF-activated endothelial cells: role of MMP-10 in VEGF-induced angiogenesis. J Cell Physiol 2010;224:734–42.
31. Tu S, Bhagat G, Cui G, Takaishi S, Kurt-Jones EA, Rickman B, et al. Overexpression of interleukin-1beta induces gastric inflammation and cancer and mobilizes myeloid-derived suppressor cells in mice. Cancer Cell 2008;14:408–19.
32. Brown C, Gaspar J, Pettit A, Lee R, Gu X, Wang H, et al. ESE-1 is a novel transcriptional mediator of angiopoietin-1 expression in the setting of inflammation. J Biol Chem 2004;279:12794–803.
33. Rudders S, Gaspar J, Madore R, Voland C, Grall F, Patel A, et al. ESE-1 is a novel transcriptional mediator of inflammation that interacts with NF-kappa B to regulate the inducible nitric-oxide synthase gene. J Biol Chem 2001;276:3302–9.
34. Sandell LJ, Xing X, Franz C, Davies S, Chang LW, Patra D. Exuberant expression of chemokine genes by adult human articular chondrocytes in response to IL-1beta. Osteoarthritis Cartilage 2008;16:1560–71.
35. Quante M, Bhagat G, Abrams JA, Marache F, Good P, Lee MD, et al. Bile acid and inflammation activate gastric cardia stem cells in a mouse model of Barrett-like metaplasia. Cancer Cell 2012;21:36–51.
36. Chen LF, Greene WC. Shaping the nuclear action of NF-kappaB. Nat Rev Mol Cell Biol 2004;5:392–401.
37. Karin M, Cao Y, Greten FR, Li ZW. NF-kappaB in cancer: from innocent bystander to major culprit. Nat Rev Cancer 2002;2:301–10.
38. Karin M, Greten FR. NF-kappaB: linking inflammation and immunity to cancer development and progression. Nat Rev Immunol 2005;5:749–59.
39. Libermann TA, Baltimore D. Activation of interleukin-6 gene expression through the NF-kappa B transcription factor. Mol Cell Biol 1990;10:2327–34.
40. Lambert PF, Ludford-Menting MJ, Deacon NJ, Kola I, Doherty RR. The nfkb1 promoter is controlled by proteins of the Ets family. Mol Biol Cell 1997;8:313–23.
41. Palayoor ST, Youmell MY, Calderwood SK, Coleman CN, Price BD. Constitutive activation of IkappaB kinase alpha and NF-kappaB in prostate cancer cells is inhibited by ibuprofen. Oncogene 1999;18:7389–94.
42. Gasparian AV, Yao YJ, Kowalczyk D, Lyakh LA, Karseladze A, Slaga TJ, et al. The role of IKK in constitutive activation of NF-kappaB transcription factor in prostate carcinoma cells. J Cell Sci 2002;115(Pt 1):141–51.
43. Lessard L, Bégin LR, Gleave ME, Mes-Masson AM, Saad F. Nuclear localisation of nuclear factor-kappaB transcription factors in prostate cancer: an immunohistochemical study. Br J Cancer 2005;93:1019–23.
44. Shukla S, MacLennan GT, Fu P, Patel J, Marengo SR, Resnick MI, et al. Nuclear factor-kappaB/p65 (Rel A) is constitutively activated in human prostate adenocarcinoma and correlates with disease progression. Neoplasia 2004;6:390–400.
45. Fradet V, Lessard L, Bégin LR, Karakiewicz P, Masson AM, Saad F. Nuclear factor-kappaB nuclear localization is predictive of biochemical recurrence in patients with positive margin prostate cancer. Clin Cancer Res 2004;10:8460–4.
46. Setlur SR, Mertz KD, Hoshida Y, Demichelis F, Lupien M, Perner S, et al. Estrogen-dependent signaling in a molecularly distinct subclass of aggressive prostate cancer. J Natl Cancer Inst 2008;100:815–25.
47. Nakanishi C, Toi M. Nuclear factor-kappaB inhibitors as sensitizers to anticancer drugs. Nat Rev Cancer 2005;5:297–309.